Search for low-mass resonances in a range between 66-110 GeV with the ATLAS detector

IOP HEPP 2025

Cheng Jiang (Edinburgh)

THE UNIVERSITY of EDINBURGH

ATLAS FUELED BY ML/AI

Begin with..

Sometimes the probabilities are very close to certainties, but they're never really certainties.

-- Murray Gell-Mann

Begin with..

Sometimes the 2.9 sigma excesses are very close to 3.0 sigma excesses, but they're never really certainties.

-- not Murray Gell-Mann

Outline

- Motivations
- Photons in ATLAS
- Analysis Strategy
- Ambiguity/Diphoton BDT
- Signal/Background Modelling
- Correction/Acceptance Factor
- Conclusion/Outlook

Motivation

Standard Model has one SU(2) doublet $\Phi = \begin{pmatrix} \phi^+ \\ \phi^0 \end{pmatrix}$

Extension to Two-Higgs-Doublet Models (2HDM)

$$\Phi_j = \begin{pmatrix} \phi_j^+ \\ (v_j + \rho_j + i\eta_j)/\sqrt{2} \end{pmatrix}, \mathrm{j} = 1,2$$

Yields 5 physical scalar (Higgs) fields: $h, H^0, A, H^\pm$

- Possible light scalars (X) in extended Higgs sector (2HDM, ALP, etc).
- CMS saw an excess (early 2.9 σ, now has lower global sig) around 95 GeV, ATLAS also observed little excess in model-dependent analysis.

HIGG-2023-12

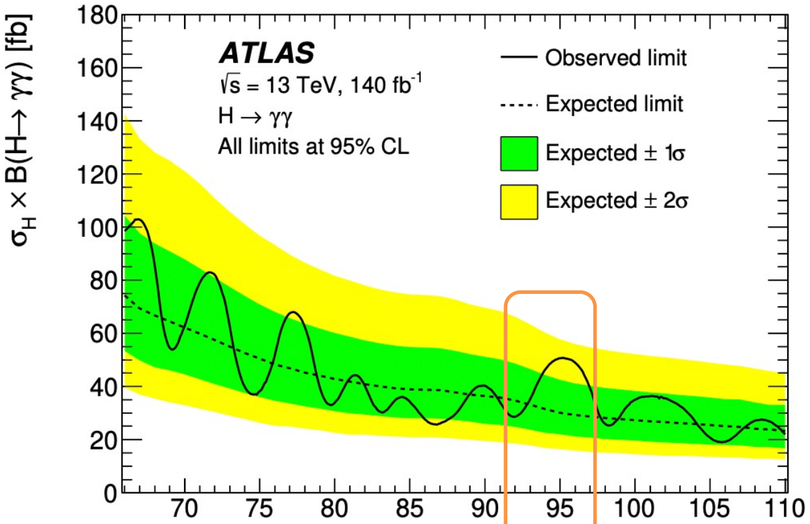

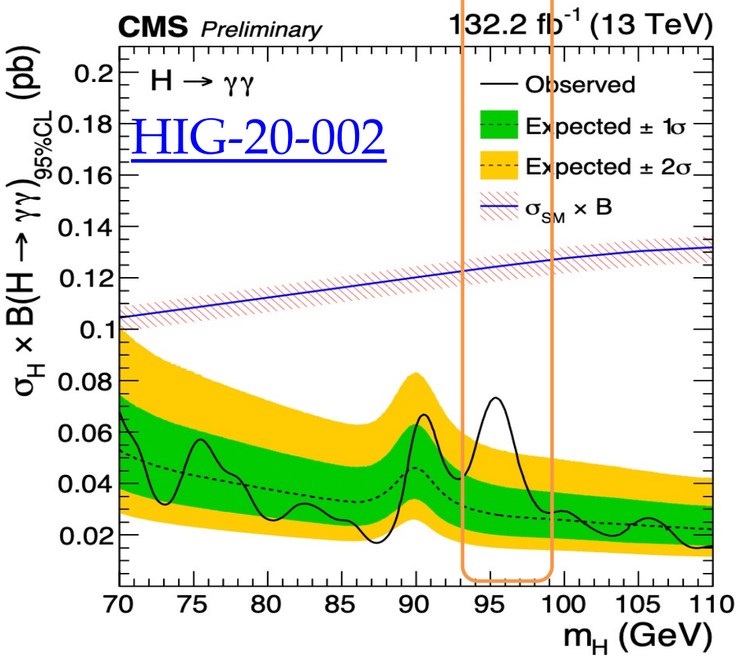

HIG-20-002

Photons in ATLAS

- Photon deposit energies in electromagnetic calorimeter cells.

- Leave a shower / “topocluster” as signatures.

Track-cluster match
➔ Electron or unconverted photon
Track-conversion vertex match
➔ Electron or converted photon

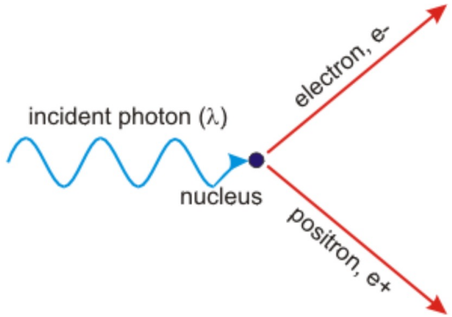

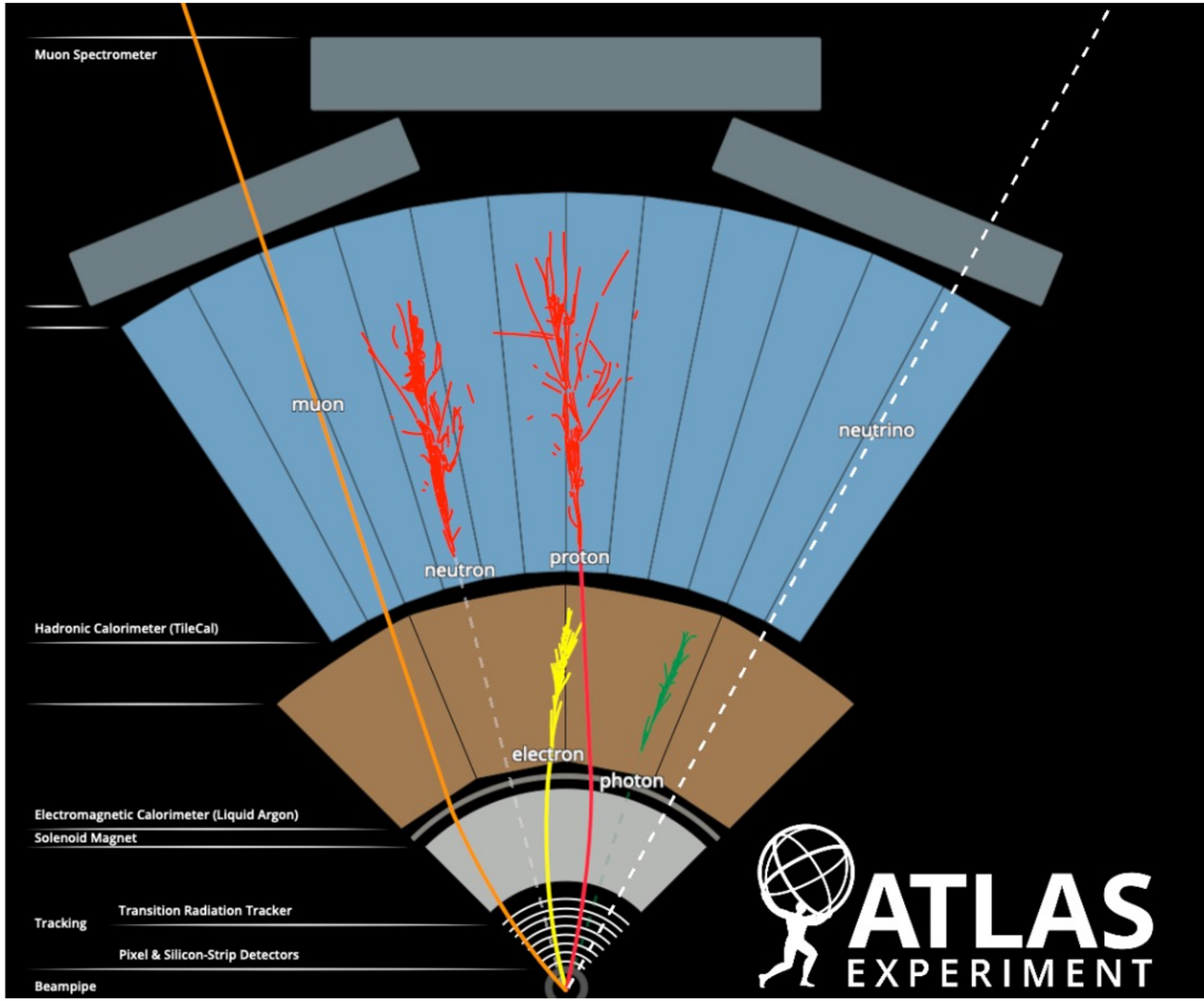

ATLAS detector schematics

Photons in ATLAS

- The "shower" shape are well described by cell energy summation over longitudinal and lateral profile.

- Those shape variables play a crucial rule distinguishing e/γ and QCD background with either cut-based or MVA methods.

Granularity of the calorimeter
➔ Define finer photon identification criteria from the shower shapes variables

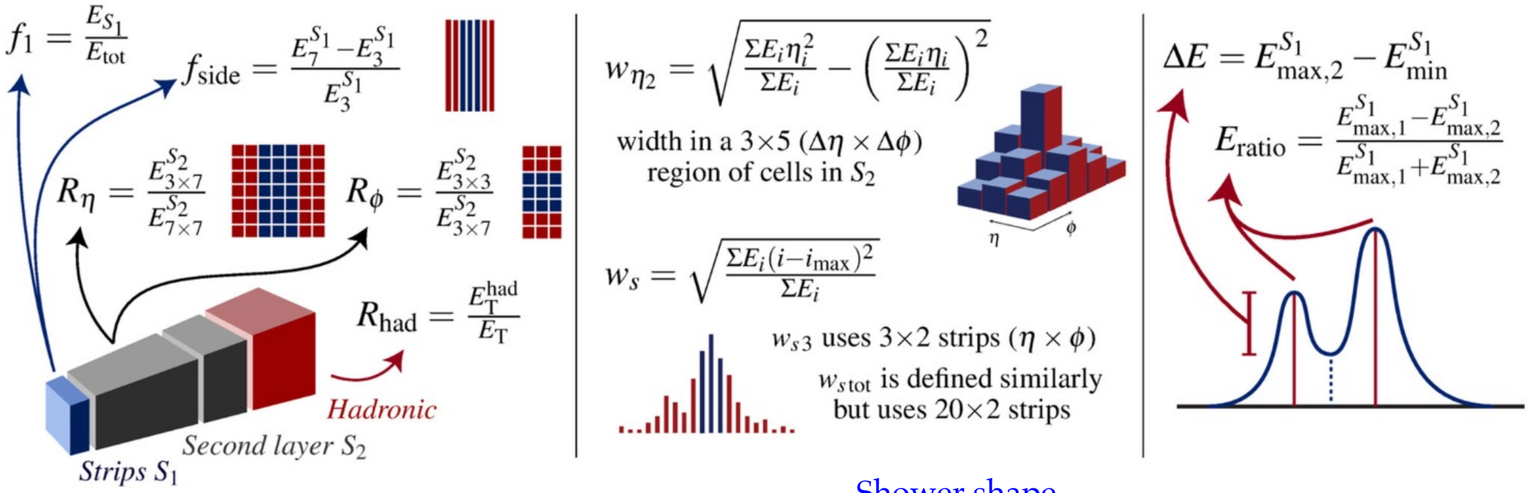

Shower shape

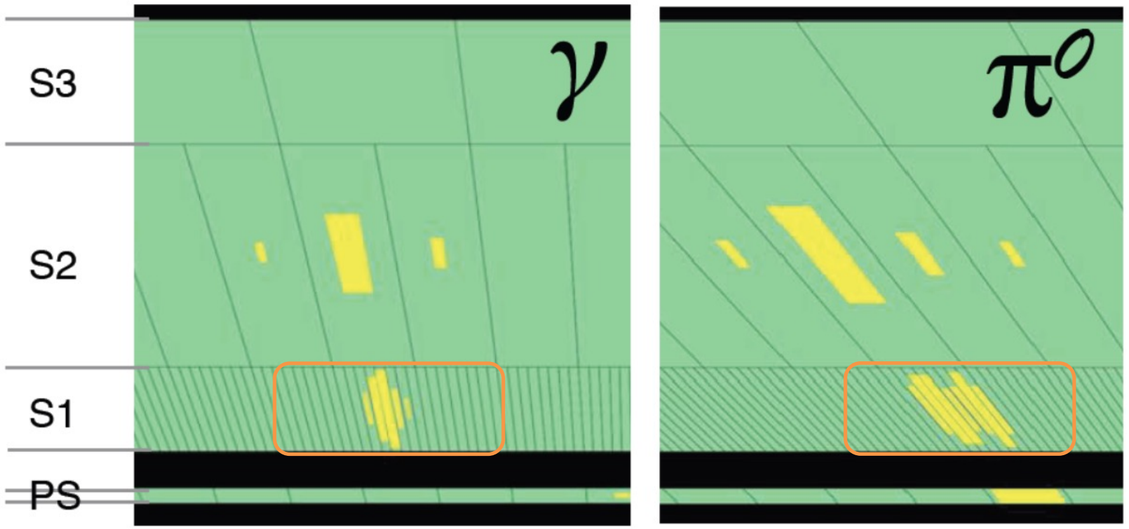

Photons in ATLAS

- Photon Calibration
- ➔ More accurate photon energy and narrow Higgs width.
- Energy corrections are applied to measured cluster energy to account for losses within the passive calorimeter material. Cell-level based transformer replacing traditional MVA, up to 40% improvement (Poster last night)

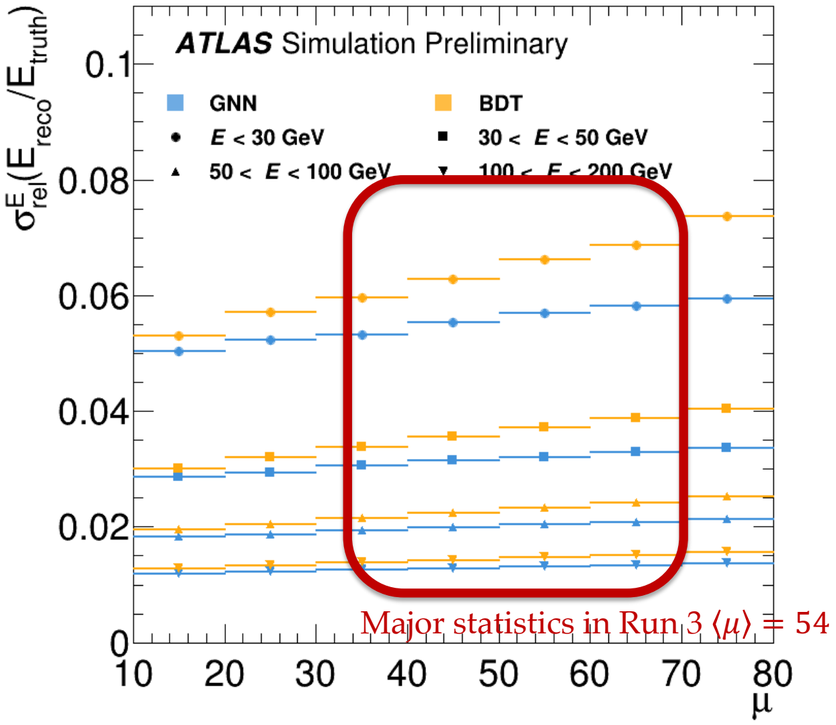

- Robust identification should have good agreement on both Data-MC. However, due to leakage or imperfect simulation, difference for photon shower shapes in Data v.s. MC. Reweighting!

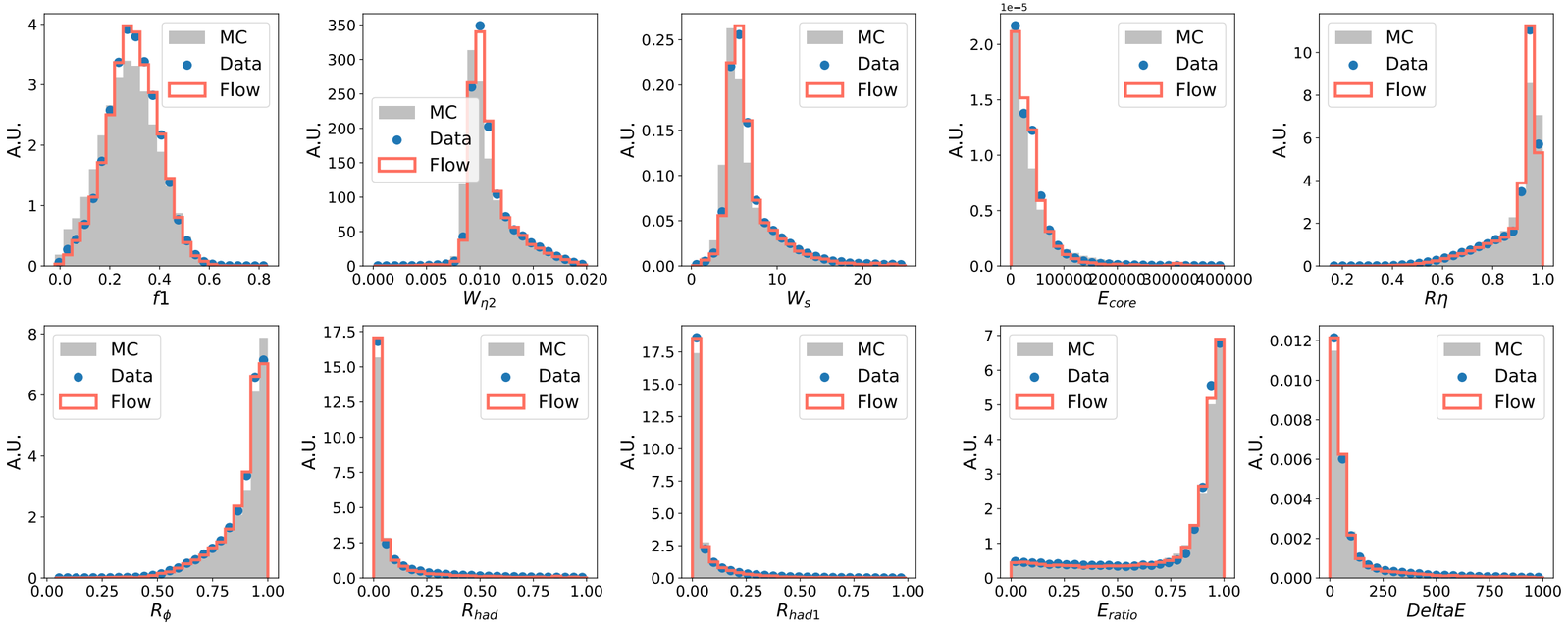

Analysis Strategy

- Direct searches for new particles, which would be detected as resonances over 66-110 GeV $\gamma\gamma$ final states. Full Run 2 ~ 140 fb-1, with partial Run 3 (2022,2023,2024) data ~ 168 fb-1.

- Three conversion categories according to photon conversion status converted (C) or unconverted (U) : UU (~52%), CU (~40%), CC (~8%).

- An additional Diphoton Classifier used to further into 3 region for each conversion (different fractions of non-resonant background and signal significance).

i. A model-independent search for a generic spin-0 scalar.
ii. A model-dependent search using a SM-like Higgs boson as a benchmark.

Analysis Strategy

- p_T> 22 GeV for both photon, identification/isolation

- Follow closely the event selection used in Run 2.
  1. Trigger/Relative p_T cut

➔ lower bound of search region, smooth falling shapes, where to fall/ "slope

  2. optimized MVA scores (cover next)
- Fit data with analytical functions that model the background and signal shape, set limits on either fiducial cross-section for generic spin-0 resonances or total cross-section for the SM-like Higgs boson.

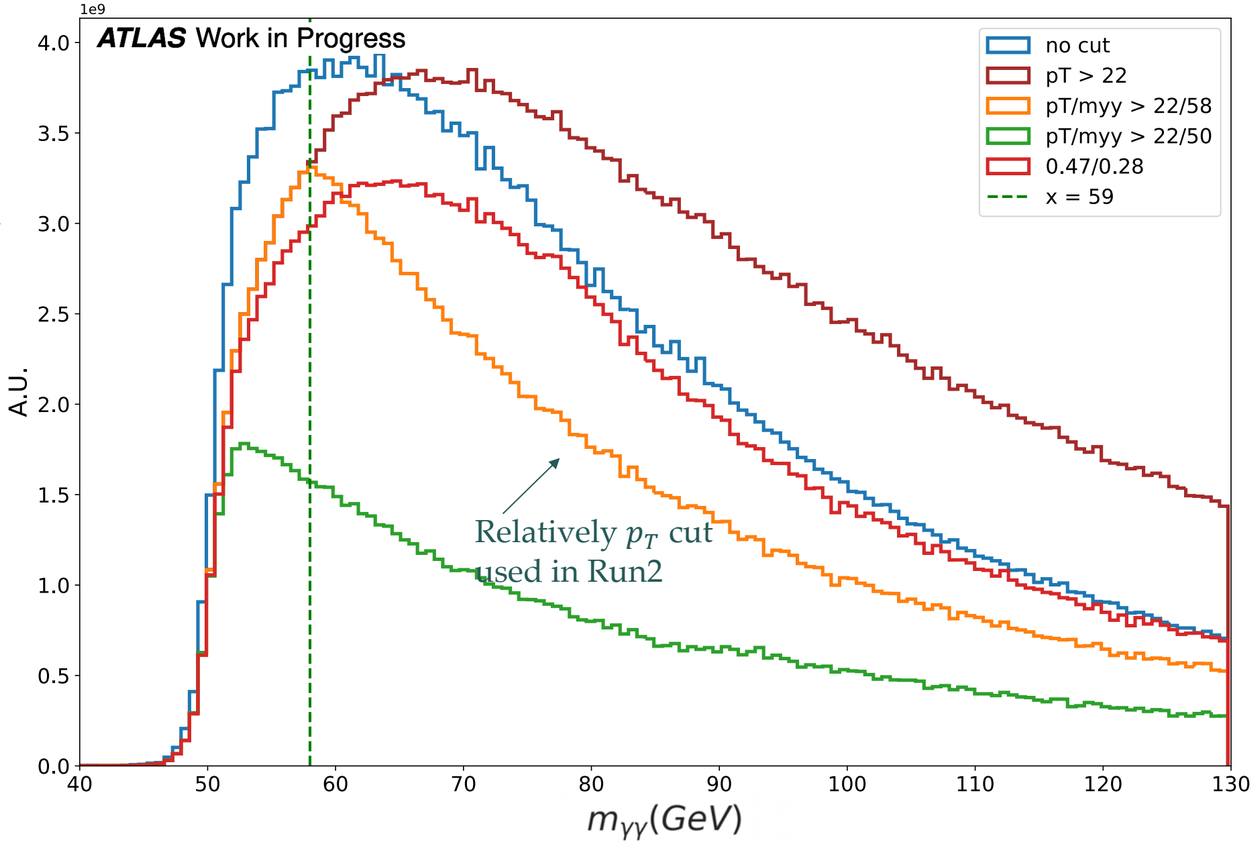

Diphoton background shapes with different relative pT cuts

Ambiguity BDT

- Gradient Boosted Decision Tree used track/cluster-level information to diminish the ambiguity between true electrons and true photons (8.7%/35% ambiguous particles).
- Clear classifier improvement over Run 2, better efficiency/fake rate trade off.
- Help supress Drell-Yan in many data control regions.

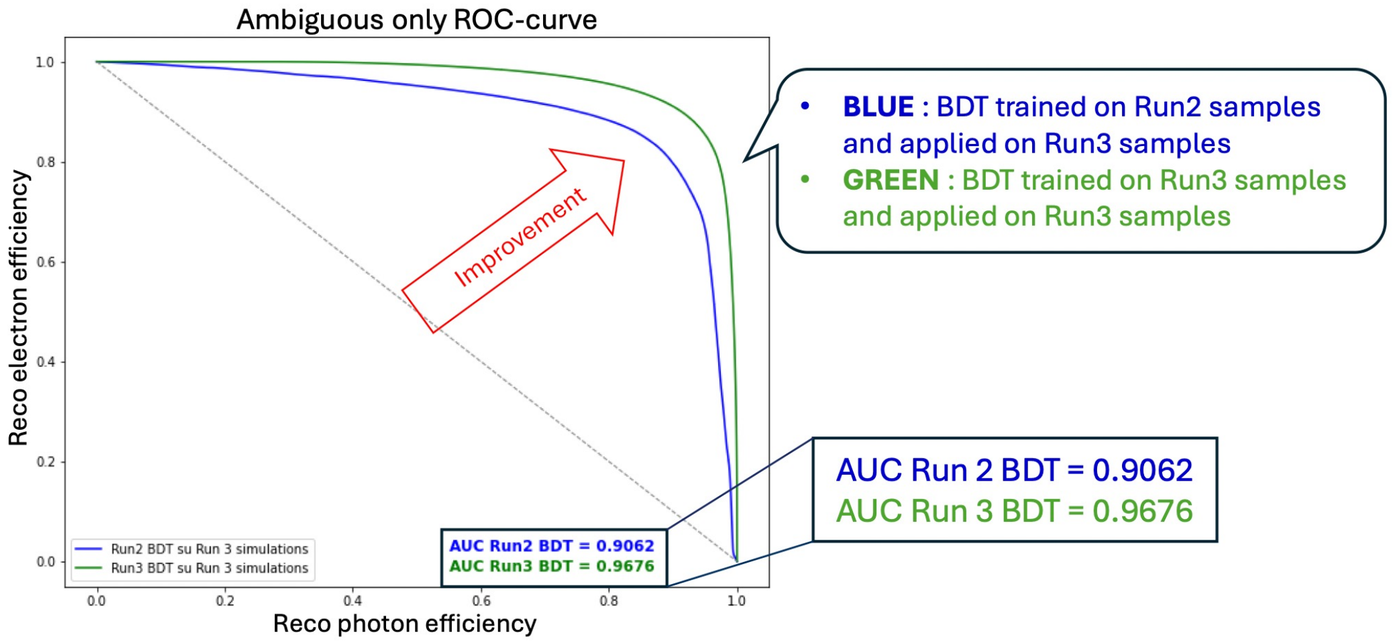

Data control region w/ Run2/Run3 BDT

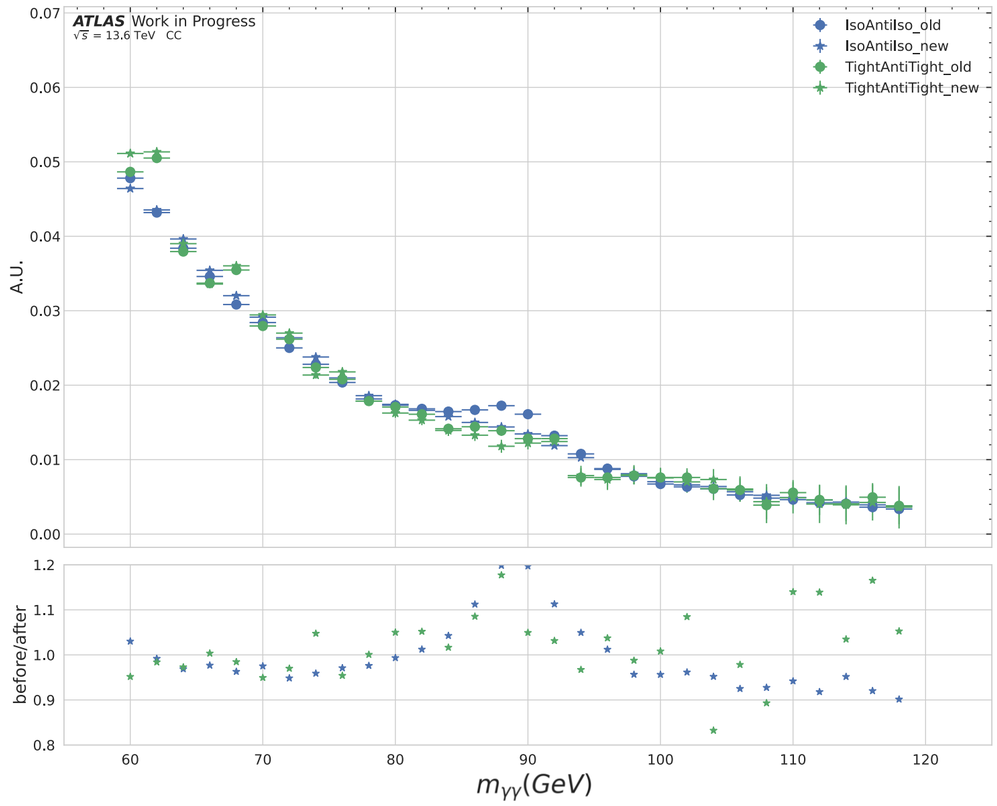

Signal Modelling

Analytical form of Double-Sided Crystal Ball (Gaussian core / asymmetric power-law tail) function is used to model narrow-width signal and detector resolution.

$$\Delta m_X = a + b \cdot m_X$$
$$\sigma_{\mathrm{CB}} = c + d \cdot m_X$$
$$\alpha_{\mathrm{low}} = e + f \cdot m_X$$
$$\alpha_{\mathrm{high}} = g + h \cdot m_X$$

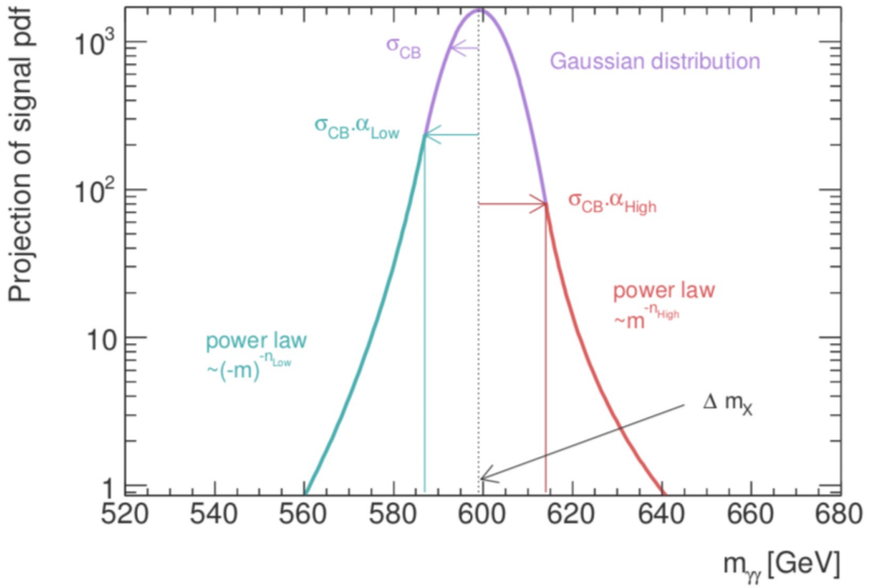

Different resonance masses, normalized entries at each signal, interpolate the parameters as the 1st order polynomial function of mass: a+b* m_X.

Simultaneously fit multiple PDF.

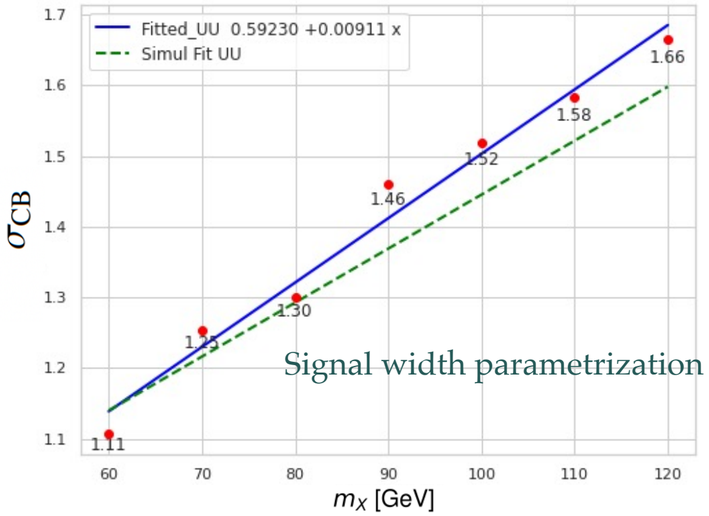

Signal modelling at 120 GeV

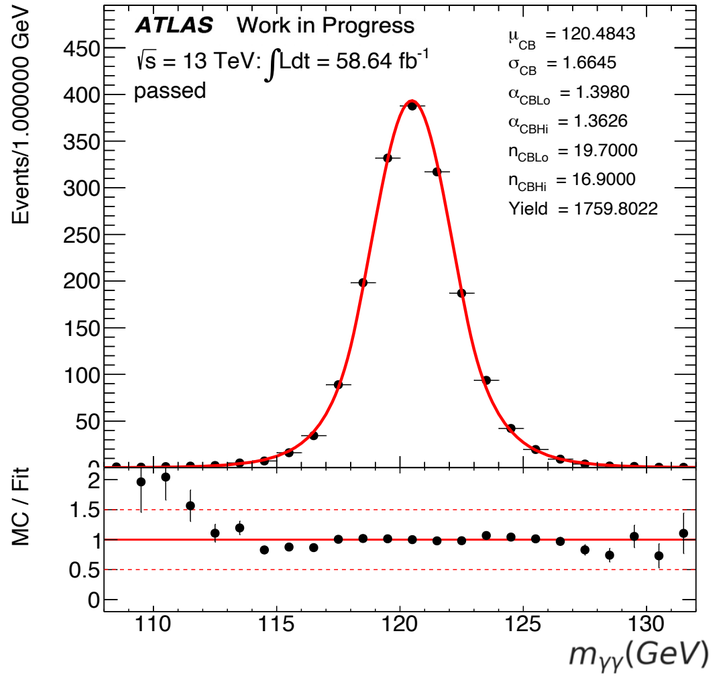

Signal Modelling

- Fit [50, 140] GeV, capture the mass dependency <-> have a better convergence on single fit.
- Inject # of signals into pseudo background data, then fit signal+background to get yields.

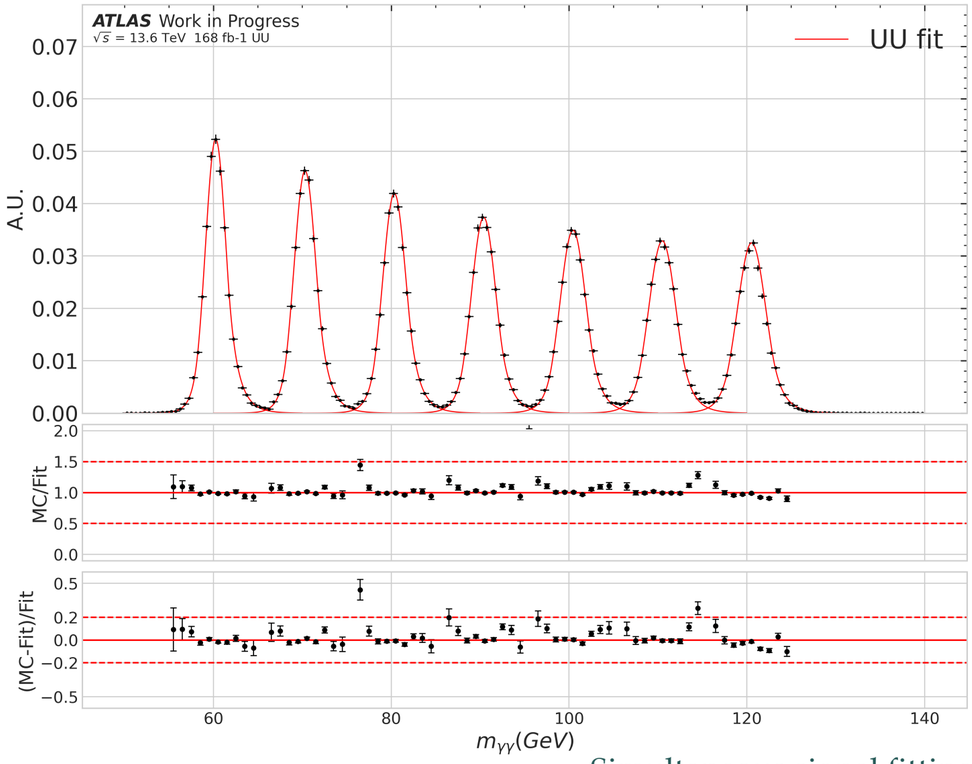

Simultaneous signal fitting

Signal injection test

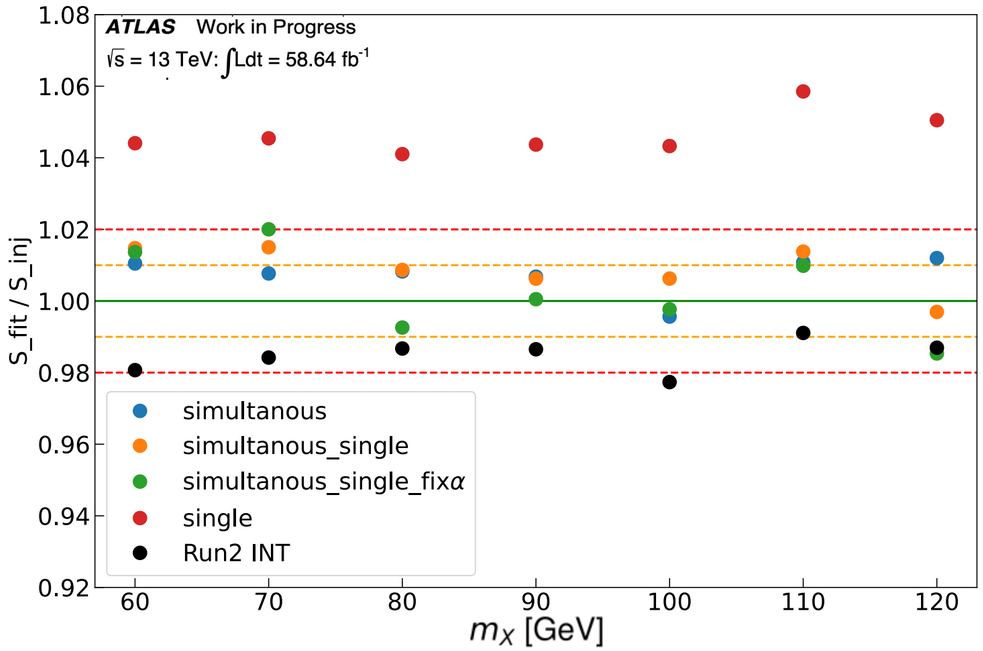

- Way to test the quality of modelling, wide scan of modelling strategy (either keep parameters fixed / floated).
- Systematics are soon to be ready.

Non resonant background

- Two main components: irreducible diphoton ($\gamma\gamma$) background from NLO QCD simulations, reducible background (yj+jj) from data control regions.

Data-driven way:

➔ background decomposition, fractions of $\gamma\gamma$ / γj / jj

control region

➔ background shape

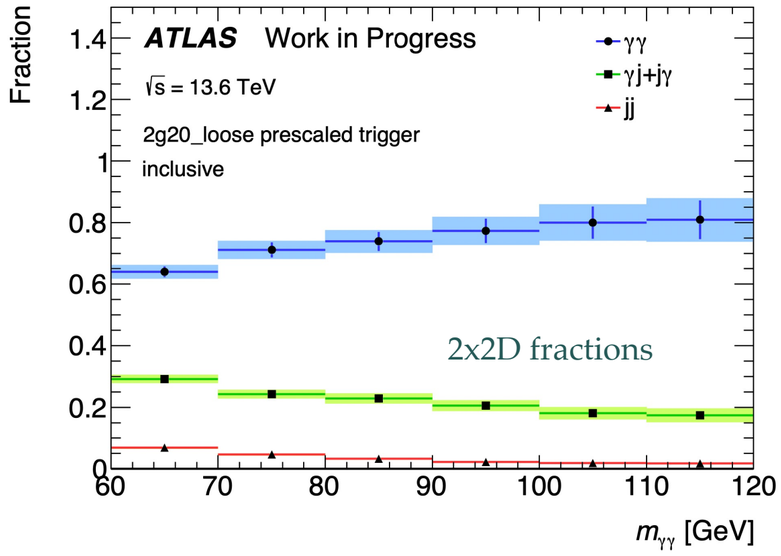

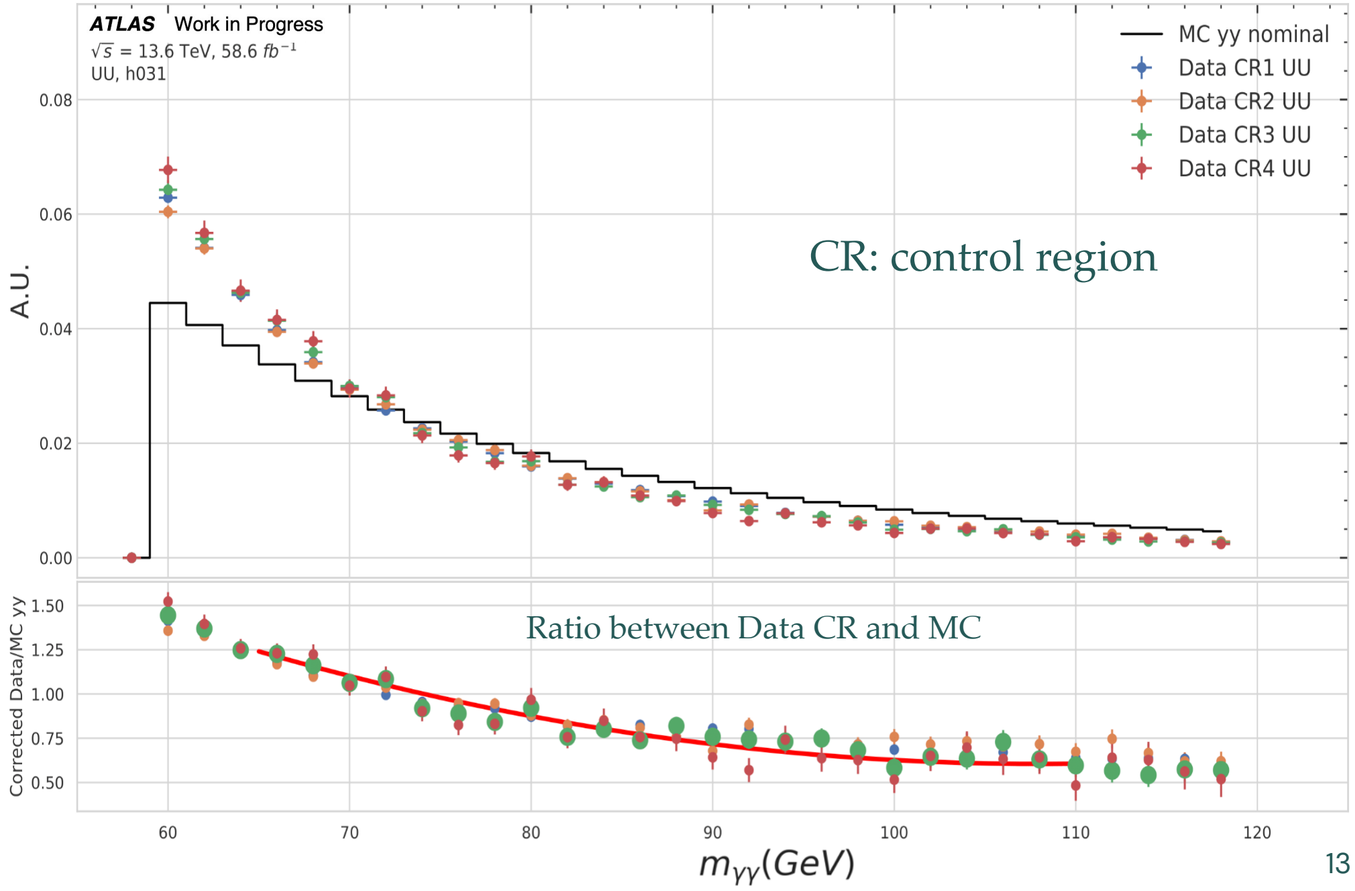

Non resonant background

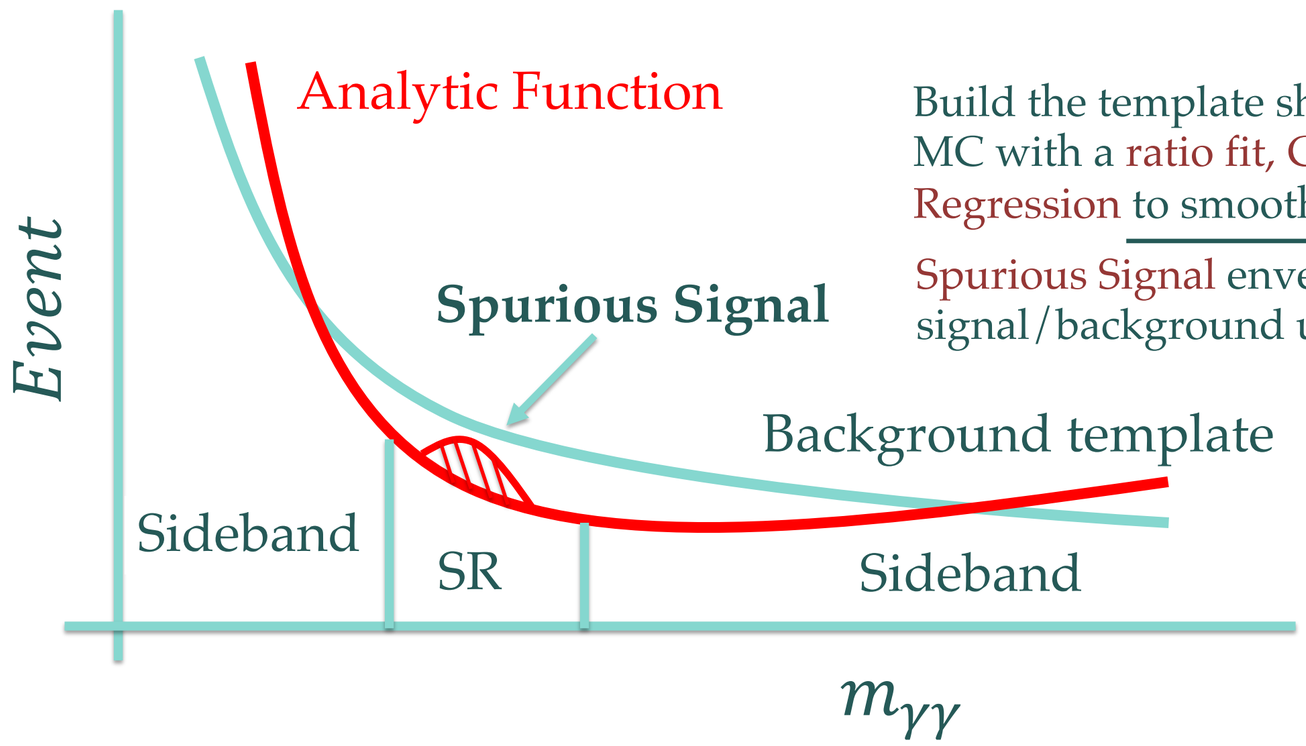

Build the template shape from pure MC with a ratio fit, Gaussian Process Regression to smooth the bin.

Spurious Signal envelope both signal/background uncertainties.

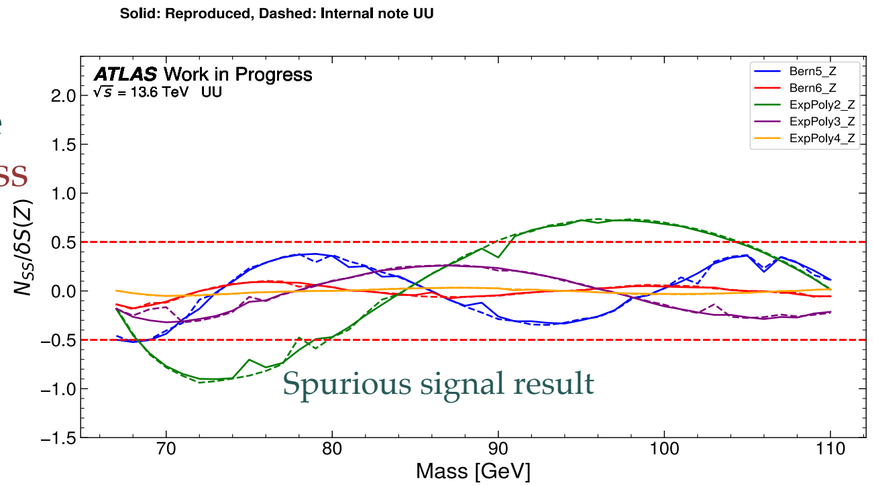

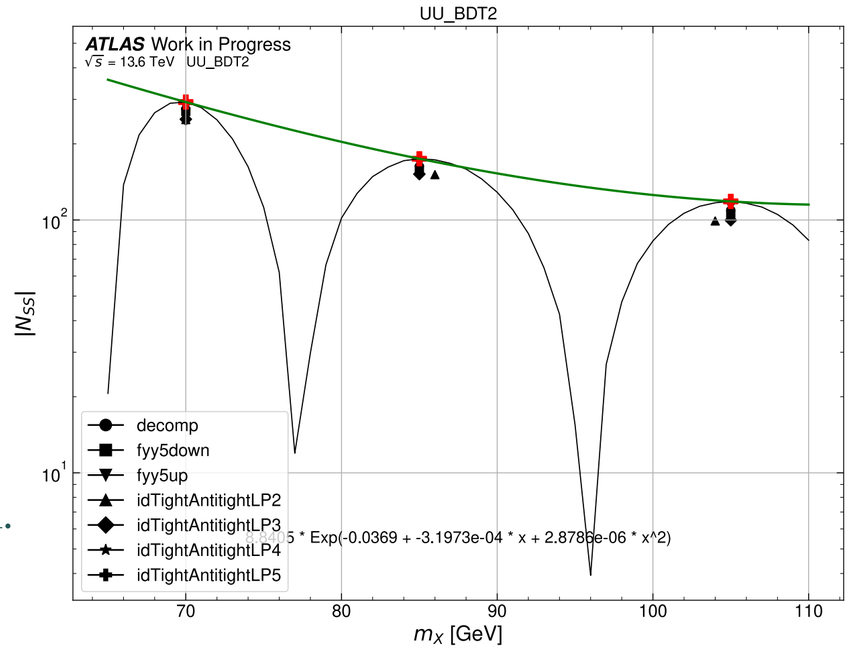

Final function form of background template

Systematics of spurious signal considering different template and choose the local maxima to fit.

Fit back the background distribution.

Correction Factor

- Bin-by-bin correction factor. (Granularity on sample ~ fitted points)
- Same selection criteria applied on reconstruction-level, truth-level selection exclude the crack region, and with 1 GeV shift on isolation cut (selection efficiency).

- For model-independent:

$$\sigma_{fid} \times \mathcal{B} = {}^{N_S}/_{C_X \mathcal{L}} \qquad C_X = {}^{N_{MC}^{sel}}/_{N_{MC}^{fid}}$$

- For model-dependent:

$$\sigma_H \times \mathcal{B} = {}^{N_S}/_{A_H C_H \mathcal{L}} \qquad A_X = {}^{N_{MC}^{fid}}/_{N_{MC}^{tot}}$$

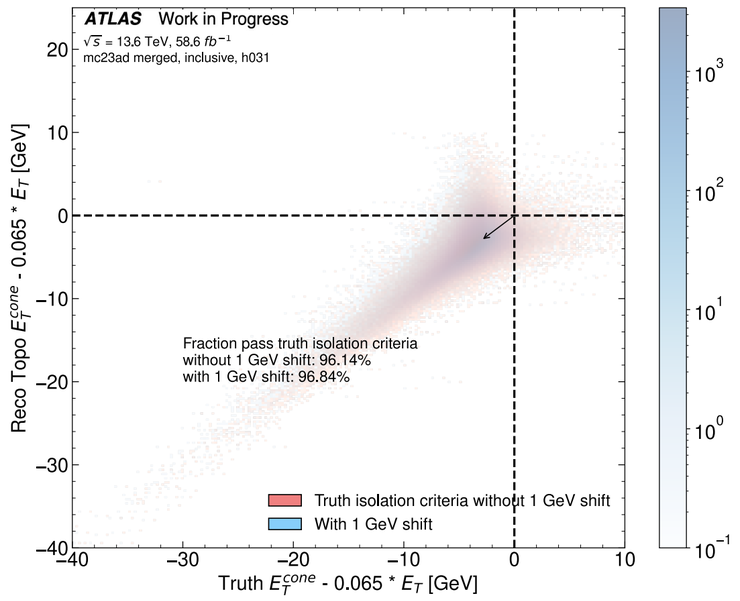

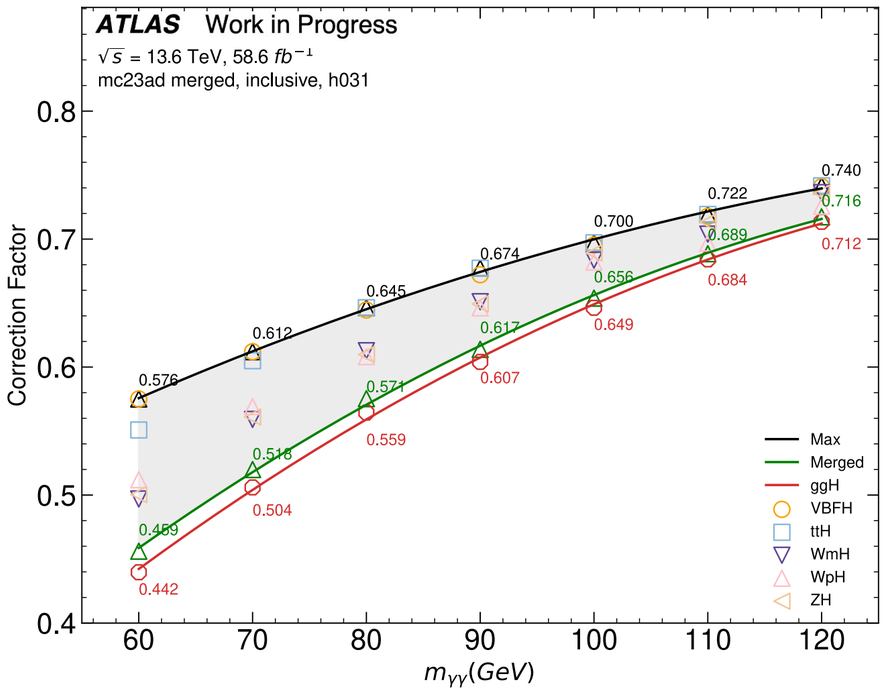

Conclusion/Outlook

- The study aims to search an additional Higgs scalar over [66,110] GeV, focusing on previous “excess” around 95.4 GeV found by both experiments.

- New MVA techniques implemented in Run3, signal/background modelling near to be finalized.

- Unblind soon, expect limit would be reduced by a factor 1.5-2 with more data and improved methods.

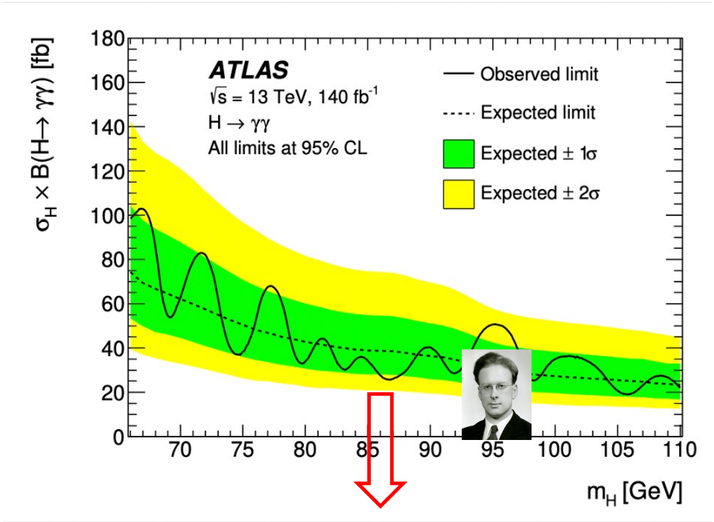

Backup

Motivation (backup)

Why Photon?

Clear signature.
Good resolution.

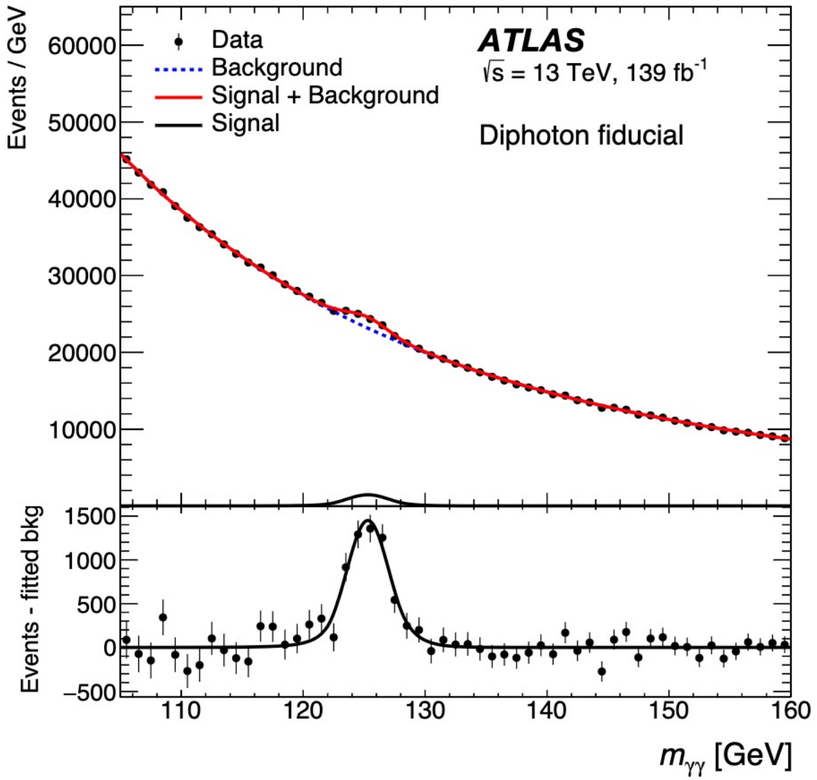

Photons in ATLAS (backup)

- Photon isolation applied on top of identification to suppress fake and brem photons. Energy flow around those backgrounds usually higher than prompt photon.

Calorimeter-based isolation (TopoEtcone20): sum of transverse energy within a cone around photon.
Track-based isolation (Ptcone20): sum of transverse momenta of tracks near around photon.

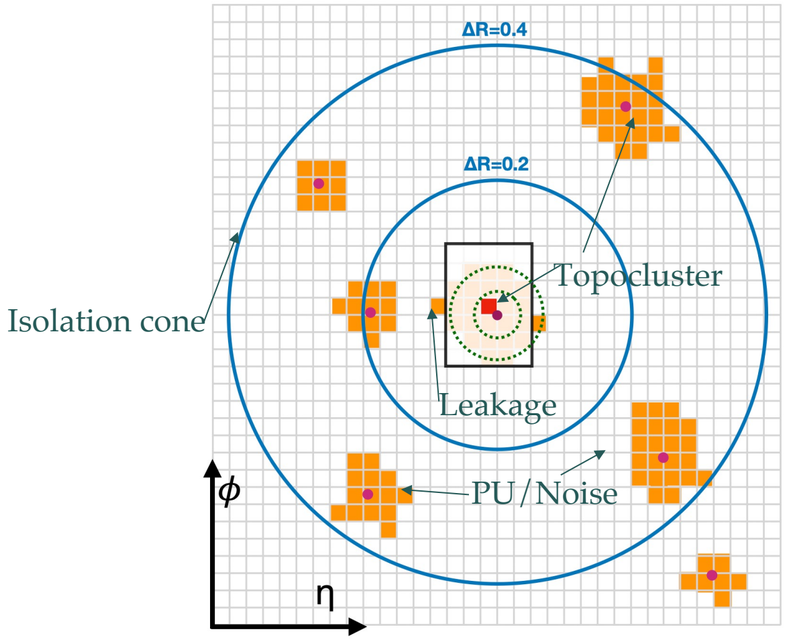

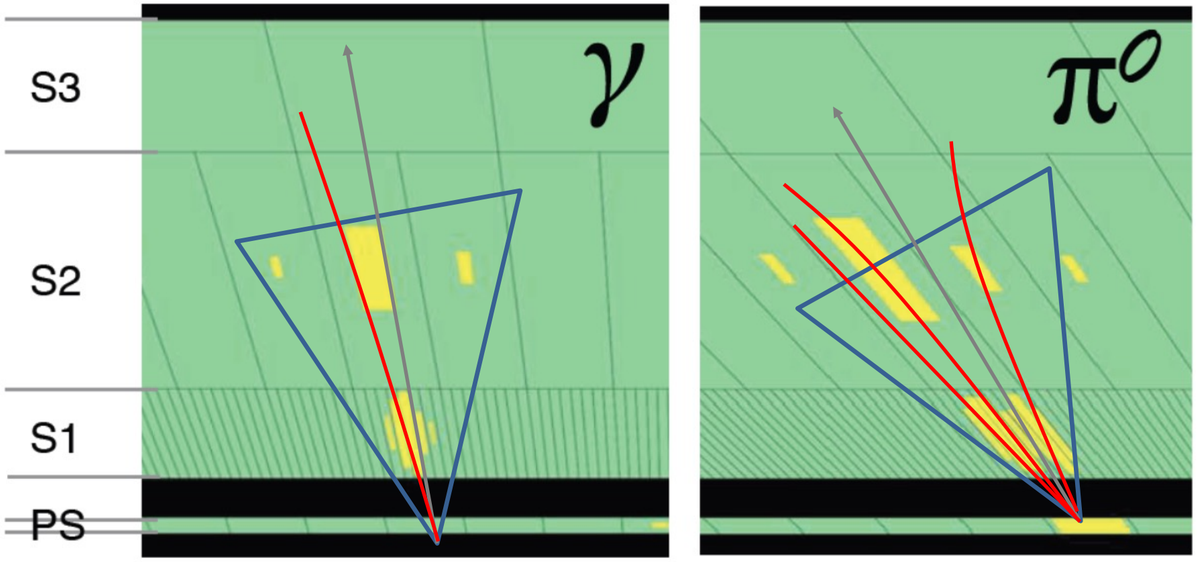

Isolation schematics

Analysis Strategy (backup)

- Signal samples: 6 different Higgs production channels (from 20 GeV to 10 GeV step size 60/70/80/90/100/110/120).
- After 2022 data-taking, using new phase-1 trigger with new Level-1 feature extractor.
- pT > 22 GeV for both photon, tight identification and relatively loose isolation requirement.

- Follow closely the event selection used in Run2.
  1. Trigger/Relative pT cut

➔ lower bound of search region, smooth falling shapes, where to fall/ "slope

  2. optimized MVA scores (cover next)
- Fit data with analytical functions that model the background and signal shape, set limits on either fiducial cross-section for generic spin-0 resonances or total cross-section for the SM-like Higgs boson.

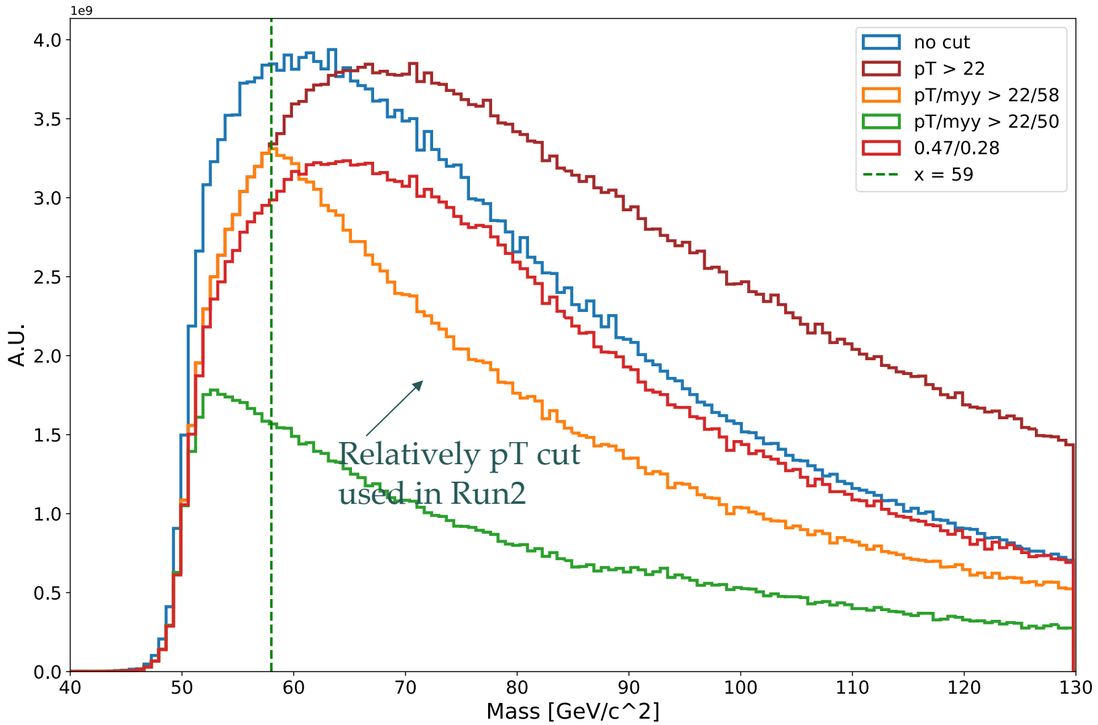

Diphoton background shapes with different relative pT cuts

Diphoton MVA

- MVA used to further categorize diphoton events, inputs from ambiguity BDT / photon kinematics. Each category splited by final score, yield different background / signal shapes and significance.
- Improvement observed over Run2.

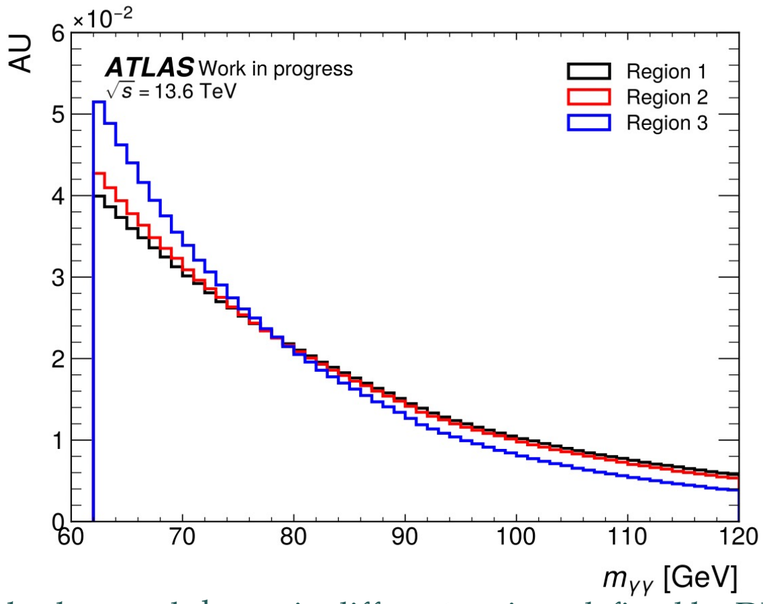

Diphoton background shapes in different regions defined by DNN

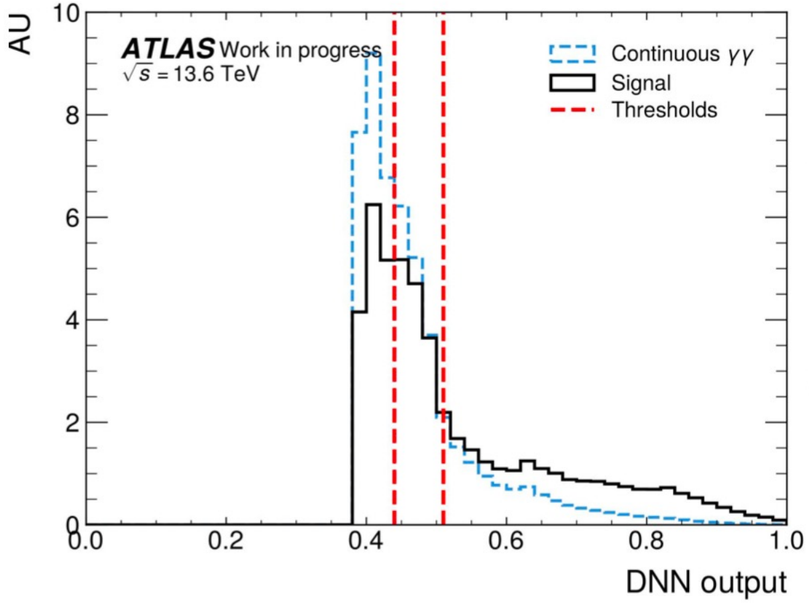

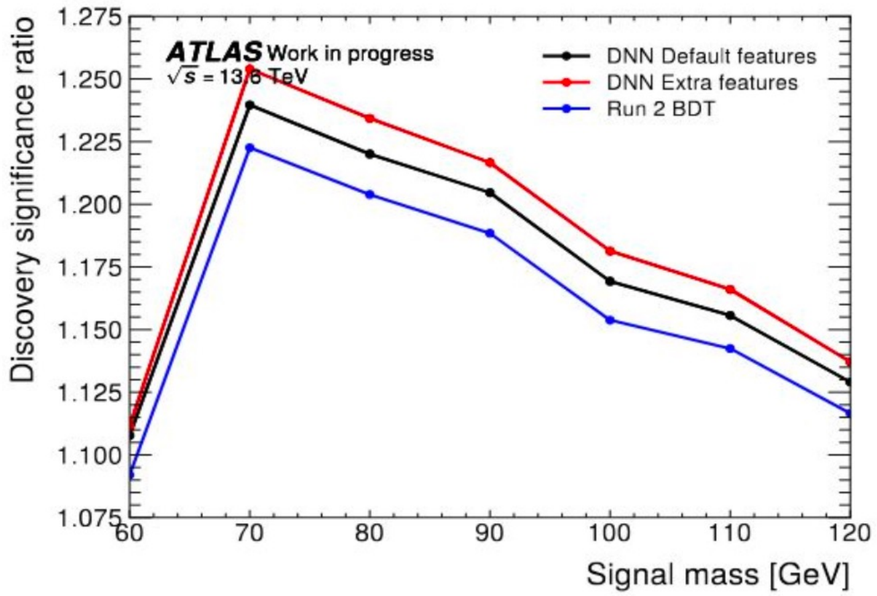

Relative sensitivity from internal notes

$\frac{f_j^{X\to\gamma\gamma}}{\sqrt{f_j^{pp\to\gamma\gamma}}}$	*Diphoton Classification*		
	Class 1	Class 2	Class 3
Photon Conversion			
UU	0.344	0.530	1.019
UC	0.314	0.536	1.028
CC	0.355	0.495	1.036

Non resonant background

- Two main components: irreducible diphoton ($\gamma\gamma$) background from NLO QCD simulations, reducible background (yj+jj) from data control regions.

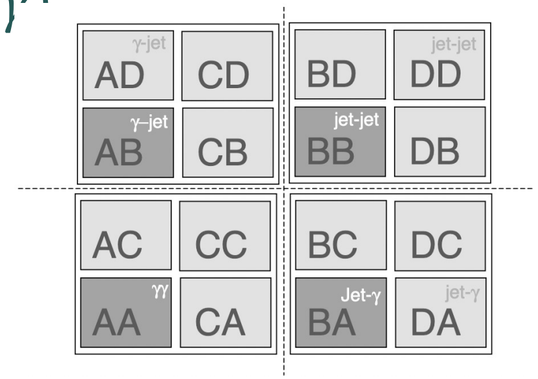

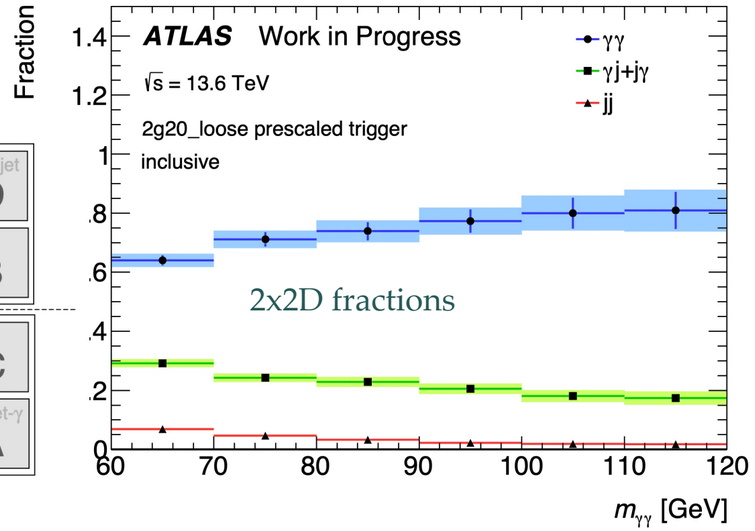

Data-driven way:

➔ background decomposition, fractions of $\gamma\gamma$ / γj / jj

control region

➔ background shape

Close to SR, large DY

CR1	γ_1	γ_2
ID	Tight	Tight
Iso	Tight	! Tight

Far away from SR

CR2	γ_1	γ_2
ID	Tight	! Tight
Iso	Tight	! Tight

CR3	γ_1	γ_2
ID	Tight	! Tight
Iso	Tight	Tight

CR4: Loose | …Loose' … | Tight

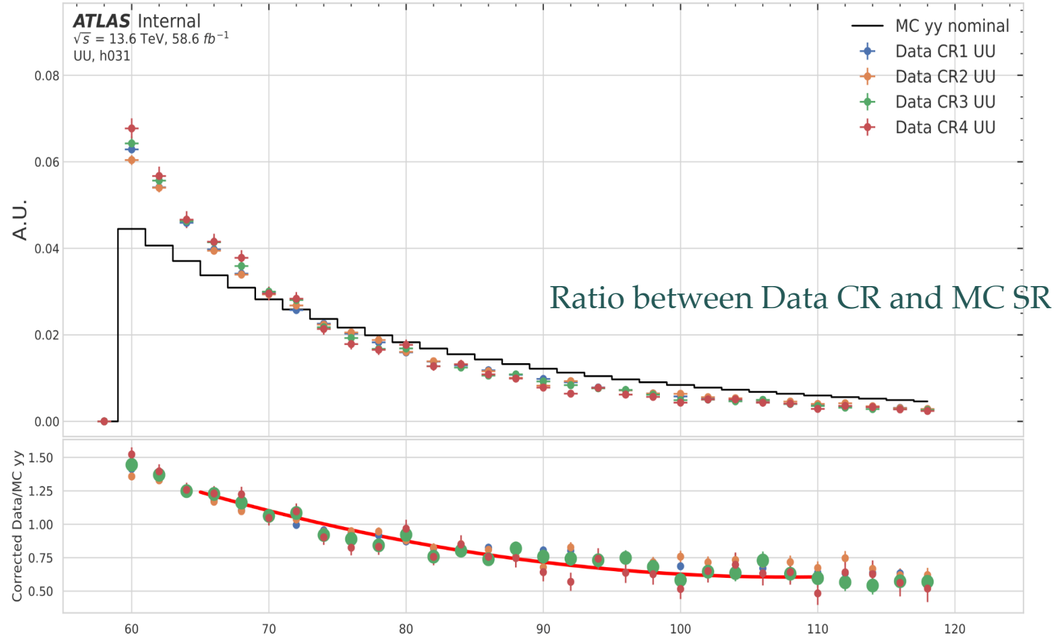

Non resonant background

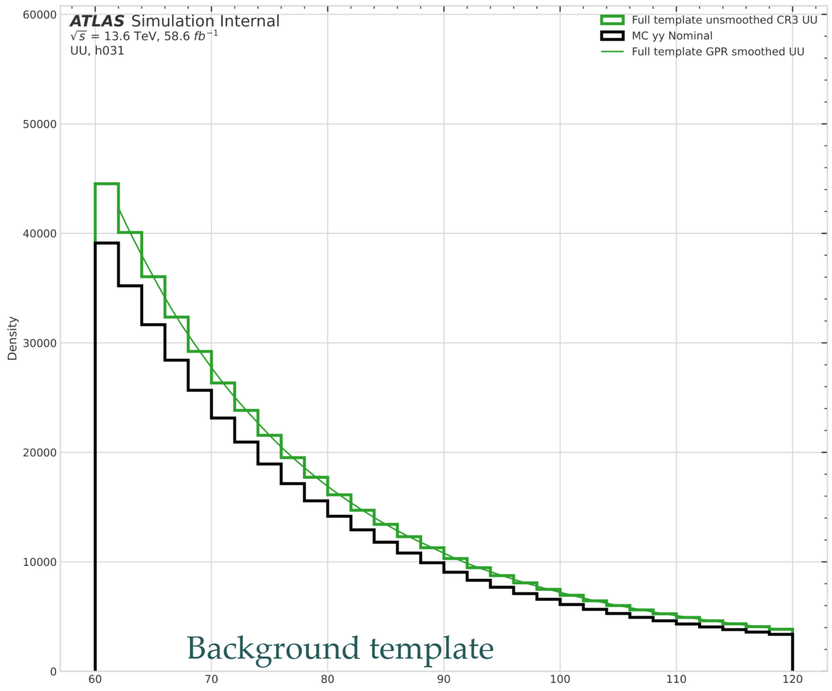

Build the template shape from pure MC with a ratio fit, Gaussian Process Regression to smooth the bin.

Spurious Signal on multiple functional form to fit background distributions with fitted signal PDF, envelope both signal/background uncertainties.

Systematics of spurious signal considering different template and choose the local maxima to fit.

Fit back the background distribution.

Final function form of background template

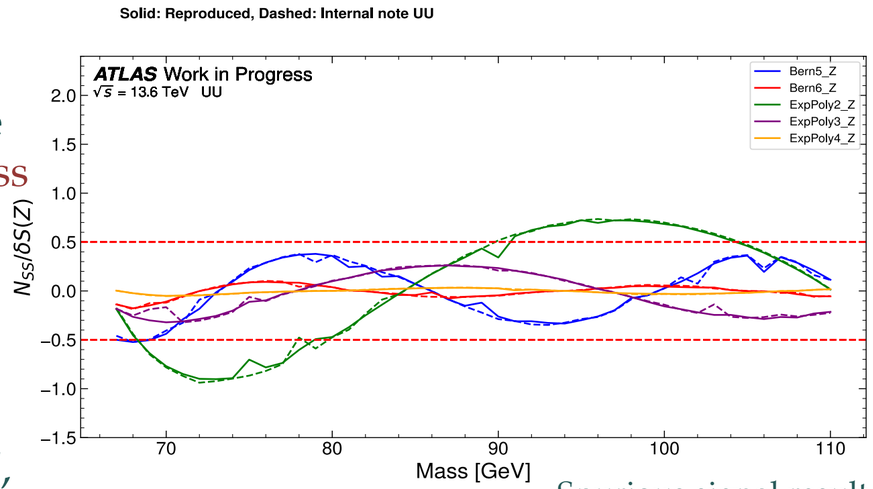

Spurious signal result

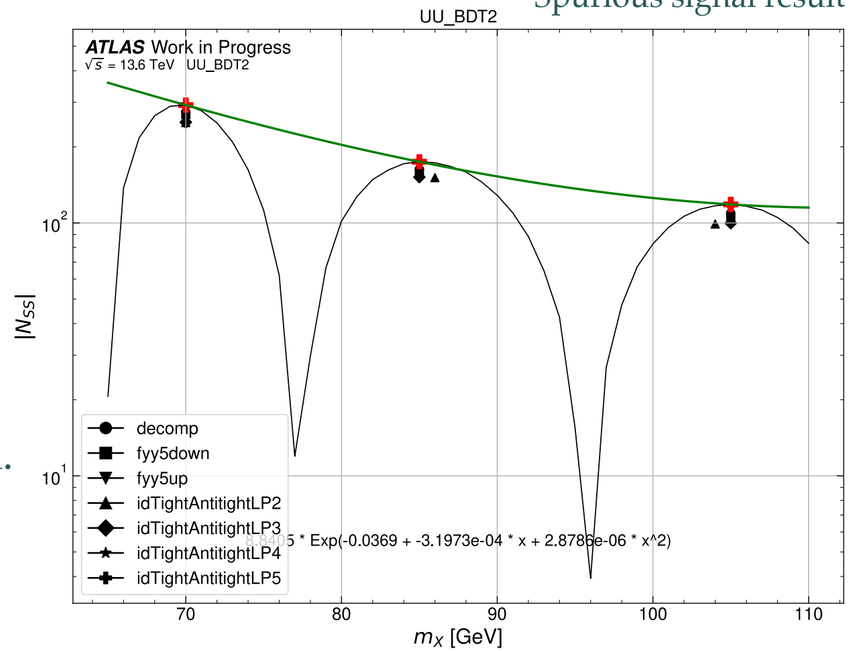

Zee background (backup)
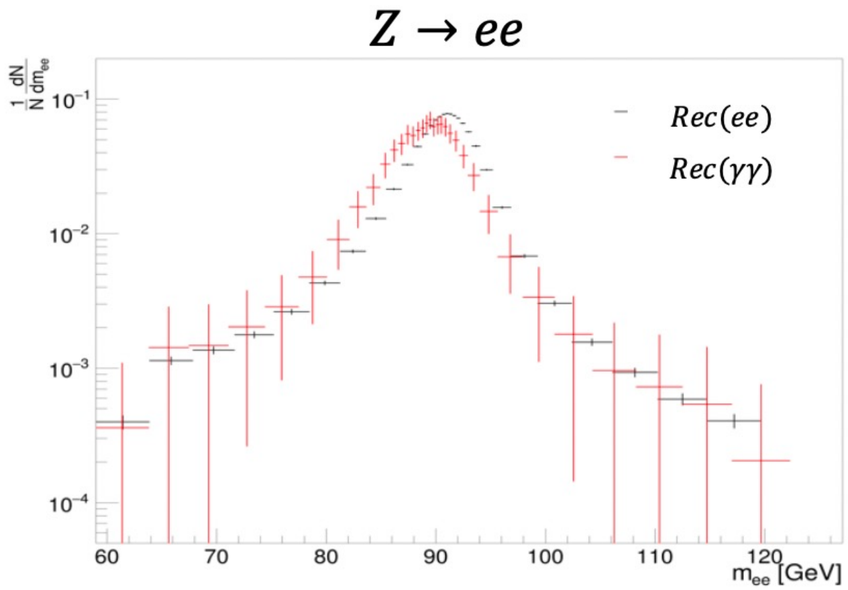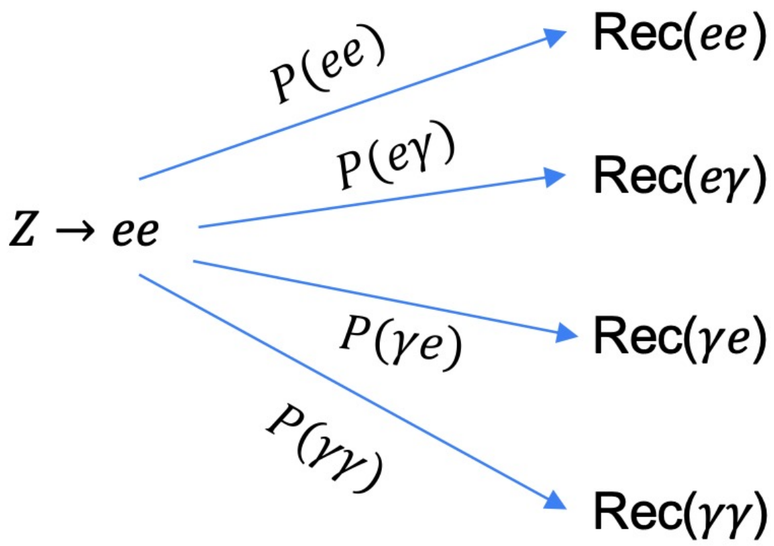
- Model/Suppress the fake photon from Drell-Yan process.
- Smirnov transformation to model difference between e and y (make an electron look like photon), shape normalization using fake rate obtained from data.